Pressure-induced phenomena in single-walled carbon nanotubes: Structural phase transitions and the role of pressure transmitting medium

C. A. Kuntscher*[,1], A. Abouelsayed[1], K. Thirunavukkuarasu[1], and F. Hennrich[2]

[1] Experimentalphysik II, Universität Augsburg, 86159 Augsburg, Germany
[2] Institute Nanotechnology, KIT, 76021 Karlsruhe, Germany

Keywords high pressure, infrared spectroscopy, single-walled carbon nanotubes, structural phase transition

* Corresponding author: e-mail christine.kuntscher@physik.uni-augsburg.de, Phone: +49 821 5983315, Fax: +49 821 5983411

1 Introduction Despite their extraordinary strength, single-walled carbon nanotubes (SWCNTs) are prone to structural phase transitions when subjected to external pressure. This has been demonstrated by numerous Raman scattering and X-ray diffraction investigations under high pressure [1–3]. Recently, it was shown that also infrared spectroscopy is a very useful experimental technique to observe the signatures of the pressure-induced deformation of SWCNTs [4–8]: The optical transitions between the Van Hove singularities in the density of states exhibit an anomaly in the pressure-induced shift at around 2 GPa, where the nanotubes change their shape from circular to oval or ellipse-like. Pressure-dependent infrared transmission studies for various pressure transmitting media [5] could also clarify that the pressure-induced anomaly is qualitatively independent of the pressure transmitting medium used.

In this paper, we present a more detailed analysis of the pressure-dependent optical data, with the focus on the high-pressure range. Furthermore, the influence of the pressure transmitting medium on the results is discussed in detail.

2 Experiment The SWCNTs were made by laser ablation technique using a 1:1 Ni/Co catalyst, and thin films of the SWCNTs (thickness $\approx$200 nm) were prepared by vacuum filtration [9, 10]. The average diameter of the nanotubes is 1.2–1.4 nm. For the purification the nanotubes were treated for 48 h in HNO_3 acid reflux; they were then suspended in dimethylformamide (DMF) and sonicated before vacuum filtration [9]. Finally, they were annealed to remove effects of the acid treatment.

The pressure-dependent transmittance was measured at room temperature in the energy range (2500–20,000 cm^{-1}) using a Bruker IFS 66v/S Fourier transform infrared spectrometer in combination with a Bruker IR Scope II infrared microscope with a 15$\times$ magnification objective. For the generation of pressures p up to 10 GPa, two types of diamond anvil cells (DACs) – a Syassen–Holzapfel type [11] and a Cryo DAC Mega from Diacell – equipped with type IIA diamonds were used. Helium, argon, CsI, and a 4:1 methanol–ethanol alcohol mixture served as pressure transmitting media. Figure 1a shows a typical view of the pressure cell loaded with a piece of carbon nanotube film marked as sample (S) together with several ruby balls (R) for pressure determination via the ruby luminescence method. The intensity $I_{sample}(\omega)$ of the radiation transmitted through the sample placed in the DAC and the intensity $I_{reference}(\omega)$ of the radiation transmitted through the pressure transmitting medium in the DAC were measured. From $I_{sample}(\omega)$ and

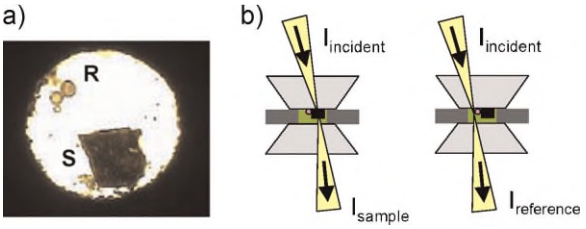

Figure 1 (online color at: www.pss-b.com) (a) Typical view of the pressure cell loaded with a piece of carbon nanotube film marked as sample (S) together with the ruby ball (R) for pressure determination. (b) An illustration of a transmission measurement configuration in a DAC.

$I_{\mathrm{reference}}(\omega)$ the transmittance and absorbance spectra were calculated according to $T(\omega) = I_{\mathrm{sample}}(\omega)/I_{\mathrm{reference}}(\omega)$ and $A(\omega) = -\log_{10} T(\omega)$, respectively. The measurement geometry is illustrated in Fig. 1b.

3 Results and discussion The background-subtracted absorbance spectra as a function of pressure are presented in Fig. 2 for different pressure transmitting media [5]. The absorption bands labeled S_{11}, S_{22}, and M_{11} correspond to interband transitions between the Van Hove singularities in the density of states. While the S_{11} and S_{22} bands correspond to interband transitions in semiconducting nanotubes, the M_{11} band corresponds to those in metallic nanotubes. The subscripts denote the sequence of the involved Van Hove singularities with increasing energy. Qualitatively, all data sets exhibit the same trend: A redshift of the interband transitions, which can be explained by deformation-induced σ^*–π^* hybridization effects and symmetry breaking [12, 13], and a band broadening with increasing pressure. The pressure-induced broadening of the absorption bands is smallest in case of helium and alcohol mixture as pressure transmitting medium because of the better hydrostaticity.

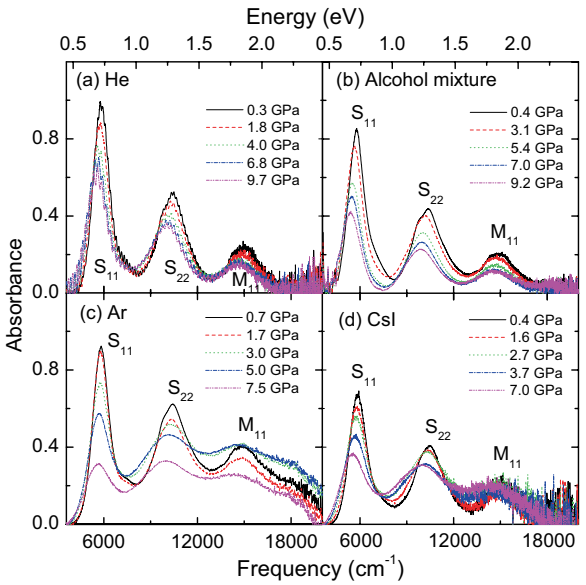

Figure 2 (online color at: www.pss-b.com) Background-subtracted absorbance spectra of purified unoriented SWCNT films as a function of pressure for various pressure transmitting media: (a) helium, (b) alcohol mixture, (c) argon, and (d) CsI. The labels S_{ii} and M_{ii} denote the optical transitions between pairs of Van Hove singularities in semiconducting and metallic SWCNTs, respectively, where the indices ii indicate the energy sequence of the involved Van Hove singularities.

Quantitative information on the pressure-induced shift of the optical transitions was obtained by fitting the background-subtracted spectra with Lorentzian functions (not shown). Due to the nanotube diameter distribution in the sample, one observes a spread in the excitation energies of the different optical transitions [14]. We can clearly resolve two Lorentzian contributions for the S_{22} transitions [labeled $S_{22}(1)$ and $S_{22}(2)$] for all pressure media. For the lower-lying S_{11} transitions the spread in energy is smaller [14] and thus not resolvable in our spectra. In case of argon and CsI as pressure transmitting medium the M_{11} band is quite broad already at lowest pressure, which excludes an unambiguous fit with more than one Lorentzian function. In contrast, for helium and alcohol mixture the broadening of the M_{11} band is considerably smaller due to better hydrostaticity, and thus two Lorentzian contributions [labeled $M_{11}(1)$ and $M_{11}(2)$] could be resolved.

The so-obtained energies of the Lorentzian functions describing the absorption features of the SWCNT film are plotted in Fig. 3 as a function of pressure. The initial values of the optical transition energies and their rates of shift under pressure for $p < p_c$ show a spread for the various pressure transmitting media [most obvious for the $S_{22}(2)$ transition], which we attribute to differences in the degree of hydrostaticity already present at low pressures. The most important result is an anomaly in the pressure-induced shift of the absorption bands: With application of pressure the optical transitions show a redshift up to the pressure $p_c =$ 2–3 GPa. Above p_c the energies of the optical transitions S_{22} and M_{11} decrease more drastically with increasing pressure, resulting in an anomaly in the pressure-induced shift at p_c. The anomaly is most obvious for helium as pressure transmitting medium, since in this case the absorption bands are narrower due to the better hydrostatic conditions, and the contributions can be better resolved. The observation of an anomaly in our data at $p_c = 2$–3 GPa for SWCNTs with diameter 1.2–1.4 nm is consistent with theoretical predictions of a structural phase transition, where the cross-section of the nanotubes changes from circular to oval or ellipse-like [15–18]. The value of p_c depends on the pressure transmitting medium used: For helium and alcohol mixture, p_c is slighly higher ($p_c \approx 3$ GPa) compared to argon and CsI ($p_c \approx 2$ GPa), which we attribute to the better hydrostaticity in case of the former two. Under better hydrostatic conditions a higher critical pressure is expected, as observed in other cases [19].

In order to clarify the role of the pressure transmitting medium for the anomaly, we present in Fig. 4 the relative

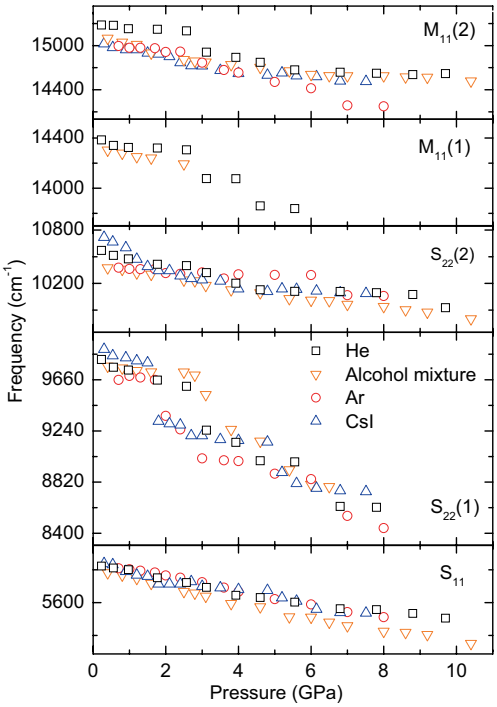

Figure 3 (online color at: www.pss-b.com) Pressure dependence of the optical transition energies obtained from the absorbance spectra, for helium (black squares), alcohol mixture (orange triangles), argon (red circles), and CsI (blue triangles) as pressure transmitting medium.

shifts of the absorption bands S_{11}, S_{22}, and M_{11} as a function of pressure for the various pressure transmitting media used. For all media we find a strong increase of the relative shifts in the pressure range 1–3 GPa. There are two important points to note: First, except for helium as pressure transmitting medium there is a spread in the critical pressure for the various optical transitions; we attribute this spread to nonhydrostatic loading conditions during the pressure runs, similar as observed in Ref. [20]. Second, the S_{11} transition does not show an anomaly and is thus not a good indicator for the pressure-induced structural phase transition, independent of the pressure transmitting medium used.

Next, we focus on the pressure-induced effects in the high-pressure range, i.e., above 4 GPa. According to Fig. 4 the shifts of the optical transitions exhibit a second anomaly at $p = 5$ GPa for CsI as pressure transmitting medium and $p = 6$ GPa in case of helium, argon, and alcohol mixture. The smaller value of the critical pressure in case of CsI is due to the less hydrostatic conditions, as described above. The finding of two anomalies is consistent with recent pressure-dependent Raman scattering results [20, 21]: Here, an anomaly in the intensity and the full-width-at-half-maximum of the radial breathing mode as well as in the shift of the tangential modes (G band) was found at ~2.5 GPa. This anomaly was interpreted as the signature for the start of a structural transition in the nanotubes, where the nanotubes' shape changes from circular to oval or ellipse-like. Furthermore, a plateau in the pressure-induced shift of the

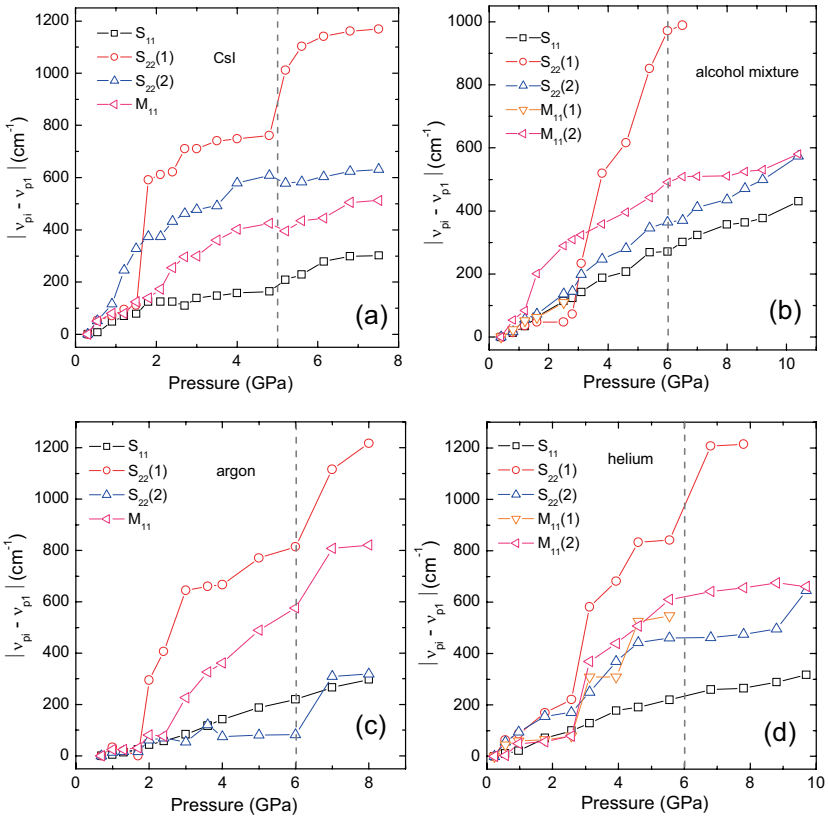

Figure 4 (online color at: www.pss-b.com) Pressure-induced energy shifts of the optical transitions with respect to the lowest pressure, calculated as the difference between the energy of the transition, ν_{p_i}, at a certain pressure p_i, and the corresponding energy at the lowest applied pressure, ν_{p_1}, for (a) CsI, (b) alcohol mixture, (c) argon, and (d) helium as pressure transmitting medium. The labels of the optical transitions are according to Fig. 3. The vertical dashed lines mark the critical pressure of the second structural phase transition.

G band was observed, with an onset at ~9 GPa, which was attributed to a more drastic change in cross-section from an ellipse-like to race-track or peanut-type shape [20, 21]. We interpret our observation of two anomalies in the pressure-induced shifts of the optical transitions in an analogous way, namely in terms of the start of the structural phase transition at $p_c = 2$–3 GPa and a more drastic deformation of the nanotubes' cross-section above 5–6 GPa.

4 Conclusions In conclusion, the pressure-induced shifts of the optical transitions in SWCNTs exhibit two anomalies, irrespective of the pressure transmitting medium used: The first anomaly occurs at a pressure $p_c = 2$–3 GPa and can be attributed to a structural phase transition, where the cross-section of the nanotubes changes from circular to oval or ellipse-like. We interpret the second anomaly at pressures 5–6 GPa in terms of a more drastic change in the nanotubes' cross-section from an ellipse-like to race-track or peanut-type shape, in agreement with recent reports on pressure-dependent Raman data [20, 21].

Acknowledgements Financial support by the DFG is gratefully acknowledged.

References

[1] S. Lebedkin, K. Arnold, O. Kiowski, F. Hennrich, and M. M. Kappes, Phys. Rev. B **73**, 094109 (2006), and references therein.
[2] J. Tang, L.-C. Qin, T. Sasaki, M. Yudasaka, A. Matsushita, and S. Iijima, Phys. Rev. Lett. **85**, 1887 (2000).
[3] S. M. Sharma, S. Karmakar, S. K. Sika, P. V. Teredesai, A. K. Sook, A. Govindaraj, and C. N. R. Rao, Phys. Rev. B **63**, 205417 (2001).
[4] K. Thirunavukkuarasu, F. Hennrich, K. Kamaras, and C. A. Kuntscher, Phys. Rev. B **81**, 045424 (2010).
[5] A. Abouelsayed, K. Thirunavukkuarasu, F. Hennrich, and C. A. Kuntscher, J. Phys. Chem. C **144**, 4424 (2010).
[6] A. Abouelsayed, K. Thirunavukkuarasu, K. Kamaras, F. Hennrich, and C. A. Kuntscher, High Pressure Res. **29**, 559 (2009).
[7] C. A. Kuntscher, K. Thirunavukkuarasu, K. Kamaras, F. Simon, and D. A. Walters, Phys. Status Solidi B **245**, 2288 (2008).
[8] C. A. Kuntscher, K. Thirunavukkuarasu, A. Pekker, K. Kamaras, F. Hennrich, M. Kappes, and Y. Iwasa, Phys. Status Solidi B **244**, 11, 3982 (2007).
[9] F. Hennrich, S. Lebedkin, S. Malik, J. Tracey, M. Barczewski, H. Roesner, and M. Kappes, Phys. Chem. Chem. Phys. **4**, 2273 (2002).
[10] F. Hennrich, R. Wellmann, S. Malik, S. Lebedkin, and M. Kappes, Phys. Chem. Chem. Phys. **5**, 178 (2003).
[11] G. Huber, K. Syassen, and W. B. Holzapfel, Phys. Rev. B **15**, 5123 (1977).
[12] J.-C. Charlier, O. Lambin, and T. Ebbesen, Phys. Rev. B **54**, R8377 (1996).
[13] G. Liu, X. Wang, J. Chen, and H. Lu, Phys. Status Solidi B **245**, 689 (2008).
[14] H. Kataura, Y. Kumazawa, Y. Maniwa, I. Umezu, S. Suzuki, Y. Ohtsuka, and Y. Achiba, Synth. Met. **103**, 2555 (1999).
[15] M. Hasegawa and K. Nishidate, Phys. Rev. B **74**, 115401 (2006).
[16] R. Capaz, C. Spataru, P. Tangney, M. Cohen, and S. Louie, Phys. Status Solidi B **241**, 3352 (2004).
[17] J. Elliott, J. Sandler, A. Windle, R. Young, and M. Shaffer, Phys. Rev. Lett. **92**, 095501 (2004).
[18] M. Sluiter and Y. Kawazoe, Phys. Rev. B **69**, 22411 (2004).
[19] C. A. Kuntscher, A. Pashkin, H. Hoffmann, S. Frank, M. Klemm, S. Horn, A. Schönleber, S. van Smaalen, M. Hanfland, S. Glawion, M. Sing, and R. Claessen, Phys. Rev. B **78**, 035106 (2008).
[20] M. Yao, Z. Wang, B. Liu, Y. Zou, S. Yu, Y. Hou, S. Pan, M. Jin, B. Zou, T. Cui, G. Zou, and B. Sundqvist, Phys. Rev. B **78**, 205411 (2008).
[21] Ch. Caillier, . D. Machon, A. San-Miguel, R. Arenal, C. Montagnac, H. Cardon, M. Kalbac, M. Zukalova, and L. Kavan, Phys. Rev. B **77**, 125418 (2008).